Published in final edited form as:
J Mol Cell Cardiol. 2010 July ; 49(1): 70–78. doi:10.1016/j.yjmcc.2009.12.013.

Tumor Necrosis Factor-α Produced in Cardiomyocytes Mediates a Predominant Myocardial Inflammatory Response to Stretch in Early Volume Overload

Yuanwen Chen, MD, PhD[1,2], **Betty Pat, PhD**[2], **Junying Zheng, PhD**[2], **Laura Cain, BS**[2], **Pamela Powell, BS, MS**[2], **Ke Shi, MD**[2], **Abdelkarim Sabri, PhD**[4], **Ahsan Husain, PhD**[2,5], and **Louis J Dell'Italia, MD**[2,3]

[1]Xinhua Hospital, Shanghai Jiaotong University School of Medicine, Shanghai, China.

[2]Center for Heart Failure Research, Departments of Medicine and Physiology and Biophysics, University of Alabama at Birmingham, Birmingham, Alabama, USA.

[3]Department of Veteran Affairs, Birmingham, Alabama, USA.

[4]Temple University School of Medicine, Pennsylvania, USA.

[5]Division of Cardiology, Department of Medicine, Emory University, Atlanta Georgia, USA.

Abstract

Acute stretch caused by volume overload (VO) of aorto-caval fistula (ACF) induces a variety of myocardial responses including mast cell accumulation, matrix metalloproteinase (MMP) activation and collagen degradation, all of which are critical in dictating long term left ventricle (LV) outcome to VO. Meanwhile, these responses can be part of myocardial inflammation dictated by tumor necrosis factor-α (TNF-α) which is elevated after acute ACF. However, it is unknown whether TNF-α mediates a major myocardial inflammatory response to stretch in early VO. In 24 hour ACF and sham rats, microarray gene expression profiling and subsequent Ingenuity Pathway Analysis identified a predominant inflammatory response and a gene network of biologically interactive genes strongly linked to TNF-α. Western blot demonstrated increased local production of TNF-α in the LV (1.71- and 1.66-fold in pro- and active-TNF-α over control, respectively, $P < 0.05$) and cardiomyocytes (2- and 4-fold in pro- and active-TNF-α over control, respectively, $P < 0.05$). TNF-α neutralization with infliximab (5.5 mg/kg) attenuated the myocardial inflammatory response to acute VO, as indicated by inhibition of inflammatory gene upregulation, myocardial infiltration (total CD45+ cells, mast cells and neutrophils), MMP-2 activation, collagen degradation and cardiac cell apoptosis, without improving LV remodeling and function. These results indicate that TNF-α produced by cardiomyocytes mediates a predominant inflammatory response to stretch in the early VO in the ACF rat, suggesting an important role of TNF-α in initiating pathophysiological response of myocardium to VO.

Keywords

tumor necrosis factor-α; myocardial inflammation; mast cells; cardiac myocytes; volume overload

Address reprints: Louis J Dell'Italia, MD, UAB Center for Heart Failure Research, Division of Cardiology, 434 BMR2, 1530 3rd Avenue South, Birmingham, AL 35294-2180, Telephone: (205) 934-3969, Fax: (205) 996-2586, loudell@uab.edu.

1. Introduction

Aorto-caval fistula (ACF) in the rat is widely employed as a model of volume overload (VO). A distinct set of myocardial responses to the stretch of early VO has been previously reported and includes cardiac mast cell accumulation and degranulation, matrix metalloproteinase (MMP) activation, and collagen degradation [1, 2]. These myocardial responses are believed to be critical in determining long term LV remodeling and outcome [3, 4]. Currently, the molecular mechanisms initiating the myocardial response to stretch in early VO of ACF have not been completely elucidated.

The distinct set of myocardial responses to stretch of early VO may be part of a major myocardial inflammatory response initiated by tumor necrosis factor (TNF)-α. TNF-α has been shown to induce myocardial inflammation which plays an important role in MMP activation and collagen degradation in pressure overload and ischemia/reperfusion [5, 6]. TNF-α is a cytokine with pleiotropic biological effects. It activates NF-κB which induces transcription of a variety of proinflammatory genes [7]. In addition, TNF-α is a potent chemoattractant for mast cells in rats and plays a role in mast cell activation and development [8]. Importantly, it has been shown to be elevated early in the LV after 24 hour ACF induction [3, 9]. Nevertheless, the cellular origin of TNF-α in early VO of ACF has been controversial [3, 9–11]. Indeed, TNF-α is a major component of mast cells but it can be potently induced in cardiomyocytes undergoing stretch [6]. In the early VO of ACF the most predominant type of stress on the LV myocardium is stretch because increased venous return is associated with a decreased arterial pressure due to the low pressure runoff into the inferior vena cava. Taken together, we hypothesize that the acute stretch caused by VO leads to a rapid induction of TNF-α in cardiomyocytes *in vivo*, which mediates a predominant myocardial inflammatory response to stretch.

To test our hypothesis, we first used microarray in conjunction with Ingenuity Pathway Analysis (IPA) to study molecular events in the LV after 24 hours of ACF. The results revealed a predominant molecular response of inflammatory genes which are linked to TNF-α. Second, we demonstrated the cardiomyocyte as a source of stretch-induced TNF-α in the myocardium. Third, we used the TNF-α antagonist infliximab, which can neutralize rat TNF-α [12], to examine the effect of TNF-α on myocardial responses to early VO after 24 hours of ACF in the rat. Our results indicate that TNF-α produced in cardiomyocytes mediates a predominant myocardial inflammatory response to stretch in the first 24 hours of ACF.

2. Materials and Methods

2.1 Reagents and antibodies

Rabbit antibodies anti-NF-κB p65, anti-phospho-NF-κB p65 (S529), anti-calsequestrin, anti-vimentin and mouse anti-heme oxygenase 1 were from Abcam (Cambridge, MA). Mouse anti-CD45 antibody, rabbit antibody anti-chemokine (c-c) motif ligand (CCL) 2, anti-myeloperoxidase and mouse anti-β-tubulin antibodies were from BD Bioscience-Pharmingen (San Jose, CA), eBioscience (San Diego, CA) and Sigma-Aldrich (St. Louis, MO), respectively. Rabbit anti-CD14 and goat anti-TNF-α antibody was from Santa Cruz Biotechnology (Santa Cruz, CA). Chemicals were purchased from Sigma-Aldrich unless otherwise indicated.

2.2 Animal experiments

This study was approved by the Animal Resource Program at the University of Alabama at Birmingham, and the investigation conforms to the Guide for the Care and Use of Laboratory Animals of NIH. ACF and sham operation were performed under sterile

conditions as previously described in our laboratory [2]. Animals were sacrificed 24 hours after operation. Echocardiography and hemodynamics were performed prior to sacrifice as previously described in our lab [2, 13]. The LV was harvested, either fixed with 10% buffered formalin phosphate, frozen in O.C.T, snap frozen in liquid nitrogen or placed in RNAlater (Ambion, Austin, TX) for future analyses. LV free wall tissue was used for studied unless otherwise indicated. For microarray analysis, 5 sham and 5 ACF rats were created. In another set of rats, sham (n=6) and ACF (n=5) rats were injected with Infliximab (5.5 mg/kg) (Remicade, Centocor, Malvern, PA) intravenously immediately after surgery. A separate group of ACF (n=6) and sham rats (n=5) were sacrificed for cardiomyocyte isolation.

2.3 Cardiomyocyte isolation

Cardiomyocytes were isolated as previously described [13]. Briefly, hearts were perfused with perfusion buffer (120 mmol/L NaCl, 15 mmol/L KCl, 0.5 mmol/L KH_2PO_4, 5 mmol/L $NaHCO_3$, 10 mmol/L HEPES, and 5 mmol/L glucose, at pH 7.0) for 5 min and digested with perfusion buffer containing 2% collagenase II (Invitrogen, Carlsbad, CA) for 30 min at 37°C. The right ventricle, atria and apex were removed before the perfused-heart was minced. The digestion was filtered, washed and cells were pelletted. Only samples with purity and viability (rod-shaped) > 95% or 80%, respectively, were used.

2.4 Collagen Volume Fraction (CVF)

Interstitial CVF was determined on picrosirius red-stained sections. Interstitial collagen was quantified as previously described [2].

2.5 MMP-2 activity

Frozen heart tissue were homogenized in extraction buffer (50 μmol/L Tris-HCl, pH 7.6, 1.5mmol/L NaCl, 0.5 mmol/L $CaCl_2$, 1 μmol/L $ZnCl_2$, 0.01% Brij 35 and 0.25% Triton x-100). Total and active MMP-2 was measured by an activity assay system according to the manufacturer's protocol (Biotrak, Amerham, Piscataway, NJ).

2.6 RNA Isolation

Total RNA was extracted from LV tissue using RNeasy Fibrous Kit (Qiagen, Maryland). Integrity of the RNA was evaluated on the Bio-Rad Experion (Bio-Rad, Hercules, CA).

2.7 Microarray Analysis

Single color microarray analysis was performed on sham and ACF rats (n=5 per group) utilizing Agilent 4×44K rat cDNA array chips (Agilent, Palo Alto CA). Data analysis was run on Genespring GX 7.3.1 (Agilent). After background subtraction, the data was normalized using 1 color scenario (Per chip, Per gene). For 'per chip normalization', all gene expression data on each single chip were normalized to the 50^{th} percentile of all values with a "present" flag only on that chip. For 'per gene normalization' the expression level of each individual gene on all chips was normalized to the arithmetic mean of that gene calculated from sham groups. ACF group was compared with sham group. A list of genes with ≥ 1.5-fold change was generated first. Following fold-change filtering, a final list was generated with significant changes in expression identified by Welch's t test with $P < 0.05$. No multiple testing correction was applied [14].

2.8 Quantitive Real-Time PCR (qRT-PCR)

qRT-PCR was performed on iCycler iQ system using SYBR green (Bio-Rad). The primers sequences are shown in Supplemental Table 1. Briefly, 500 ng total RNA was reverse-transcribed in a 20 μl reaction volume using an iScript cDNA synthesis kit (Bio-Rad).

Samples were run in duplicate and copy numbers were acquired according to serial dilution of standards. GAPDH was used as an internal control.

2.9 Ingenuity Pathway Analysis

Differentially expressed genes were uploaded onto IPA 6.0 (http://www.ingenuity.com) to identify significantly perturbed biological networks. Biological networks were generated according to the function interaction among genes in the uploaded data set. Calculated P-value determines the probability that these genes may show up together in the network by chance alone.

2.10 Histopathological analysis

Mast cell and neutrophils were identified using Giemsa staining [13] or anti-myeloperoxidase (1:50) antibody [15] on paraffin sections respectively. Positive cells were counted throughout the LV free wall and expressed as number of cells/mm^2. Frozen sections were used for immunohistochemical detection of CD45+ cells. Sections were fixed in acetone (−20°C), blocked at room temperature and then incubated with anti-CD45 antibody (1:100) overnight at 4°C. After that, sections were incubated with FITC-conjugated secondary antibodies. Nuclei were stained with DAPI (Vector). Positive cells were enumerated on all the fields (10 to 20) along epicardium of the LV free wall at × 400 magnification.

2.11 TUNEL assay

The TUNEL assay was performed on paraffin-embedded sections using the DeadEnd fluorometric TUNEL kit (Promega, Madison, WI). TUNEL-positive non-myocytes were counted throughout the LV free wall and expressed as number/mm^2.

2.12 Western blot

80 μg of tissue or cell lysate was separated on 4–12% Bis-Tris gradient gel (Invitrogen), transferred to a PVDF membrane then incubated with antibody to CD14 (1:1000), TNF-α (1:500), CCL2 (1:1000), SMAD family member 7 (1:1000), heme oxygenase 1 (1:500), Vimentin (1:1000), phospho-NF-κB p65 (1:500) or total NF-κB p65 (1:1000) overnight at 4°C followed by incubation with HRP-conjugated secondary antibodies. Membranes were incubated with Chemiluminescent Substrate (Pierce, Rockford, IL) and exposed to X-ray film. Bands were quantified by Scion Image 4.0.3. β-tubulin (1:4,000) and calsequestrin (1:2000) antibodies were used as internal controls for tissue and cardiomyocytes lysates respectively.

2.13 Statistics

Data are expressed as mean ± SEM. CD45+ cells, mast cells, MMP-2 activity, CVF and TUNEL-positive non-myocytes were analyzed by ANOVA (ACF vs. sham, with or without TNF-α blockade) followed by Post Hoc Student-Newman-Kuels analyses. Student's t-test was used for echo, hemodynamics, qRT-PCR and western blot data analyses and correlation was determined using Pearson correlation. A $P < 0.05$ was considered statistically significant.

3. Results

3.1 Microarray identifies a predominant early inflammatory response in the LV after ACF

Twenty-four hour ACF induced a marked increase in LV end-systolic pressure (LVEDP) and LV end-diastolic dimension (LVEDD) in ACF vs. shams, demonstrating a significant VO and stretch on the LV (Table 1). Compared to shams, ACF had 141 upregulated and 21

downregulated transcripts (fold-change ≥ 1.5, $P < 0.05$). There was excellent correlation between microarray and qRT-PCR ($P < 0.001$) (Figure 1, A and B).

Functional classification of differentially expressed genes indicated a cluster of genes involved in inflammation (Figure 1C). These genes included cytokine/chemokines, growth factors, transmembrane receptors, post-receptor signaling proteins and transcription factors — which are involved in the regulation, activation, chemotaxis, attachment and proliferation of leukocytes (Table 2). We also found a marked increase in several inflammation suppression genes, such as interleukin 1 receptor antagonist and interleukin 22 receptor antagonist and heme oxygenase 1 (Table 2). However, the mRNA of three major proinflammatory cytokines of TNF-α, interleukin 1β and interleukin 6, were not changed according to microarray, and this was confirmed by qRT-PCR (Figure 1D).

We next explored the functional interactions among the altered genes using IPA. IPA identified a gene interactive network of 28 altered genes which were confirmed by qRT-PCR with the exception of integrin β6 (Figure 2A, Table 2). The biological functions of this network were characterized by inflammation and immune response. At the central point of this network was NF-κB. This was confirmed by a 2.3-fold increase in phospho-NF-κB p65 (phosphoserine-529, a site phosphorylated by TNF-α) in ACF vs. sham (Figure 2B). TNF-α can potently augment NF-κB activation. Therefore, utilizing IPA, we assessed the biological connection between genes in this network and TNF-α. Indeed, IPA demonstrated that of the 28 genes in this network, 19 have been reported to be directly regulated by or are regulators of TNF-α (Figure 2C). In addition, western blot on four well-known TNF-α related inflammatory response proteins in the identified IPA network (Figure 2A) : chemokine (c-c) motif ligand 2 (CCL2) (chemokine), CD14 (receptor), SMAD family member 7 (intercellular signaling molecular), and heme oxygenase 1 (oxidative stress related) confirmed significant increases of these four proteins in ACF over shams (Figure 3, A–D).

3.2 Enhanced TNF-α production in LV tissue and cardiomyocytes

The microarray and IPA findings indicated TNF-α as an inflammatory mediator in acute VO. Although TNF-α mRNA was unchanged, there was a 1.7-fold increase in both pro- and active LV TNF-α in ACF vs. shams (Figure 4A). We isolated cardiomyocytes from sham and ACF rats to determine whether TNF-α was produced by cardiomyocytes. We found a 2-fold increase in pro-TNF-α and a 4-fold increase in active TNF-α in ACF cardiomyocytes (Figure 4B). The purity of cardiomyocytes was documented by the lack of vimentin (Figure 4C).

3.3 Effects of TNF-α antagonist, infliximab, on inflammation

We next explored the effect of TNF-α on the early inflammatory response in the heart after ACF. Leukocytes and/or mast cell infiltration are major components of inflammation. There was a 2-fold increase in CD45+ cells including neutrophils and mast cells in the LV free wall of untreated ACF vs. sham rats (Figure 5, A–F), which were suppressed by TNF-α neutralization (Figure 5, A–C).

TNF-α can promote leukocyte infiltration by inducing chemokine (c-x-c) motif ligand 1 (CXCL1) and CCL2 [7]. CXCL1 did not show up in microarray data according to our filtering criteria. A retrospective check of the original data indicated a 1.78-fold change of CXCL1 with P-value of 0.08. This was verified by qRT-PCR (1.74-fold, $P = 0.07$) (Figure 5G). CCL2 expression increased according to the microarray and was verified by qRT-PCR in ACF rats (Figure 5H). Both CCL2 and CXCL1 were attenuated by TNF-α blockade (Figure 5, G and H).

Furthermore, the effect of TNF-α blockade on all altered inflammatory genes in the IPA network was verified by qRT-PCR.TNF-α blockade suppressed the upregulation of 20 (out of 28) genes in the IPA network (Figure 3C), including important pro-inflammatory mediators of TNF-α, such as CCL2, chemokine (c-c) motif ligand 7, chemokine (c-x-c) motif ligand 12, colony stimulating factor 1 and integrin αL (Figure 3C). Genes that were not significantly or partially influenced by infliximab included interleukin 1 receptor antagonist which could be activated through alternative mechanisms, genes situated upstream of TNF-α production (CD14, CD32), genes indirectly or partially regulated by TNF-α (Versican, chemokine (c-x-c) motif ligand 11), and genes negatively regulated by TNF-α (solute carrier family 7 member 1, TNF-α-induced protein 6). In addition, infliximab reduced genes involved in oxidative stress (heme oxygenase 1) and apoptosis (B-cell CLL/lymphoma 3) (Figure 3C). These data implicated TNF-α as a key mediator of the LV inflammatory response in VO of ACF.

3.4 Effects of TNF-α blockade on MMP-2 activation and collagen degradation

TNF-α induced inflammation plays an important role in MMP activation and collagen degradation [16, 17]. We found a >2-fold increase in active MMP-2 without a significant increase in total MMP-2 in untreated ACF vs. sham rats (Figure 6A). This was associated with 44% decrease in interstitial collagen (Figure 6B). Infliximab abrogated MMP-2 activation and collagen degradation in ACF rats (Figure 6, A and B).

3.5 Effects of TNF-α blockade on cardiac cell apoptosis

Cardiac cell apoptosis also occurs in TNF-α induced myocardial inflammation [6, 16]. Apoptotic cardiomyocytes were rarely seen in the heart of sham or ACF rats with or without infliximab administration (0–3 per heart) at this early time point. However, ACF caused a 57% increase in TUNEL- positive non-myocytes vs. sham, and this was significantly attenuated by infliximab (Figure 6, C–E).

3.6 Effects of TNF-α blockade on LV remodeling and function at 24 hours ACF

At 24 hours, TNF-α blockade had no effect on LV weight/BW, lung weight or heart rate in shams or ACF. However, TNF-α blockade decreased LVESP in both sham and ACF rats with no attenuation of increased LVEDP and LVEDD. LV fractional shortening and velocity of circumferential wall shortening did not increase in ACF treated with TNF-α blockade, despite a decrease in LVESP (Table 1).

4. Discussion

Here we show that in the VO of acute ACF in the rat, there is an intense inflammatory response to stretch in addition to mast cell infiltration, MMP activation and collagen degradation, all of which are mediated through TNF-α. Further, the cardiomyocyte itself is a significant source of TNF-α in acute VO. Despite a complete abrogation of these events, TNF-α neutralization does not improve LV remodeling and function at this early time point.

Inflammation in early ACF is previously implied by several studies which show an increase in mast cells or several major pro-inflammatory cytokines including TNF-α, interleukin 1β and interleukin 6 [3, 9, 18]. To our knowledge, this study is the first to demonstrate the mechanism by which acute ACF produces an intense myocardial inflammatory response. Given the absence of pathogens, sepsis, or ischemia/reperfusion in this model, the intensity of this inflammatory response of the pure stretch of VO is unexpected.

TNF-α has been shown to be a potent inducer of cardiac inflammation, MMP activation and collagen degradation in TNF-α knockout/over-expression animal models of pressure

overload, ischemia/reperfusion, or virally-induced myocarditis, as well as exogenous infusion of TNF-α to normal animals [5, 6, 19]. The current study demonstrates a comparable response in acute VO, suggesting similar myocardial responses to TNF-α regardless of etiology. Thus, the potent effect of TNF-α in early VO may in part explain the rapid decrease in interstitial collagen, that is detected as early as 12 hours in this model [2].

Many cells types in the myocardium can produce TNF-α under stress, in particular mast cells. As a rapid response of the host defense system, mast cells degranulate and release pre-stored TNF-α which in turn induces further production of TNF-α and other inflammatory factors in constitutional cells and other inflammatory infiltrates. This cascade of events initiates and perpetuates the inflammatory response in myocardial infarction [20], ischemia/reperfusion [21] and sepsis [22]. However, in the absence of these pathological stimuli in VO, the stimulus for TNF-α production could be cardiomyocyte stretch alone, as manifested by an increase in LVEDP and LVEDD in the absence of an increase in mean arterial pressure. Stretch causes activation of the TNF-α transcription factor NF-κB and TNF-α production in cardiomyocytes *in vitro* [6, 23]. Although elevated TNF-α protein is not accompanied by increased mRNA at 24 hours, the identification of a 2- fold increase in pro-TNF-α in ACF cardiomyocytes vs. shams strongly indicates local production of TNF-α rather than uptake from the circulation [10]. One explanation for this discrepancy is that TNF-α mRNA increases rapidly (within one hour) after acute stretch of cardiomyocytes [6] and is only transiently upregulated in acute VO in vivo [24]. In addition, protein can persist for a long time after an injury even when mRNA induction is lost. The presence of active TNF-α with a relative abundance of pro-TNF-α within the cardiomyocytes suggests gradual and persistent activation of pro-TNF-α after a transient induction of mRNA. However, a later and further increase may be due to other cell types such as mast cells and fibroblast [3, 25].

Our results also show that TNF-α controls neutrophils and mast cell infiltration in early VO of ACF. Neutrophils can cause MMP activation and collagen degradation through increased oxidative stress or release of proteases such as cathepsin G. Indeed, we recently reported that blockade of cathepsin G attenuates collagen degradation and cardiac cell apoptosis [15]. Furthermore, neutrophil infiltration and activation can be induced by TNF-α directly or through the chemokine, CCL2, both of which are elevated after 24 hours of ACF.

Mast cells have been recognized as an important effector in early VO. Mast cells numbers increase rapidly in early VO [4], however, the factors that control their differentiation and accumulation are complex. Nevertheless, the current study demonstrates that TNF-α mediated mature mast cell accumulation in early VO. Indeed, TNF-α is a potent chemoattractant for mast cells in rats [8], and is required for tissue mast cell development and survival in response to stem cell factor [26]. Collectively, these findings are in accordance with our data suggesting that TNF- α is a major cytokine responsible for mast cell chemoattraction and/or maturation in early VO.

Despite a complete abrogation of inflammatory events, LV remodeling and function is not improved at 24 hours by TNF-α neutralization. This finding is understandable because we find no adverse LV remodeling or functional changes at 24 hours of ACF in rats. It is tempting to speculate that the abrogation of inflammation and collagen loss with TNF-α neutralization may translate into improved function long term. However, TNF-α neutralization also blocked the acute induction of cytokines including CCL2 and colony stimulating factor 1, heme oxygenase 1 and osteoprotegerin, which can protect cardiomyocytes from hypoxic stress and may be beneficial in the setting of increased myocardial oxygen consumption in VO [27–29]. Collectively, our results suggest that TNF-α can be detrimental or cardioprotective on cardiac remodeling and function. This

contention is supported by a recent finding showing divergent effects of two different TNF-α receptors (TNFR) on TNF-α mediated myocardial remodeling and inflammation, which in the case of TNFR1 is detrimental or alternatively cardioprotective with TNFR2 [30]. The relative level of these two receptors may vary with the stress type and disease stage, and thus TNF-α neutralization may not be uniformly beneficial in all causes and stages of heart failure. This may explain the recent findings that TNF-α neutralization by etanercept initiated 3 days before or 3 weeks after creation of ACF improved diastolic dysfunction at 3 weeks or 8 weeks respectively, but only LV eccentric remodeling in the latter [31]. Taken together, the pleitropic effects of TNF-α coupled with the potential variable expression of its newly recognized receptors may explain the failure of clinical trials examining the efficacy of TNF-α inhibition in Class III and IV heart failure, which included patients with stable, late stage heart failure from both ischemic and nonischemic etiologies [3, 6, 32].

In summary, our findings demonstrate, for the first time, that stretch of VO activates cardiomyocyte production of TNF-α which mediates an intense myocardial inflammatory response in early VO of ACF. Whether this inflammatory response waxes and wanes or persists throughout the course of VO is an open question. Further, TNF-α effects are differently translated into pathophysiological outcomes through two different types of receptors and the relative levels of the receptors may vary with disease stage. Therefore, these emerging concepts must be explored before targeting TNF-α in the treatment of VO.

Supplementary Material

Refer to Web version on PubMed Central for supplementary material.

Acknowledgments

This study is supported by National Heart, Lung and Blood Institute Grants RO1 HL54816, National Heart, Lung and Blood Institute Grant Specialized Centers of Clinically Orientated Research grant in Cardiac Dysfunction P50HL077100 (to L.J.D), and partially by National Nature Science Foundation of China No. 30971263 (to Y.C).

References

1. Brower GL, Janicki JS. Pharmacologic inhibition of mast cell degranulation prevents left ventricular remodeling induced by chronic volume overload in rats. J Card Fail. 2005; 11:548–556. [PubMed: 16198252]
2. Ryan TD, Rothstein EC, Aban I, Tallaj JA, Husain A, Lucchesi PA, et al. Left ventricular eccentric remodeling and matrix loss are mediated by bradykinin and precede cardiomyocyte elongation in rats with volume overload. J Am Coll Cardiol. 2007; 49:811–821. [PubMed: 17306712]
3. Levick SP, Gardner JD, Holland M, Hauer-Jensen M, Janicki JS, Brower GL. Protection from adverse myocardial remodeling secondary to chronic volume overload in mast cell deficient rats. J Mol Cell Cardiol. 2008; 45:56–61. [PubMed: 18538342]
4. Brower GL, Chancey AL, Thanigaraj S, Matsubara BB, Janicki JS. Cause and effect relationship between myocardial mast cell number and matrix metalloproteinase activity. Am J Physiol Heart Circ Physiol. 2002; 283:H518–H525. [PubMed: 12124196]
5. Kubota T, McTiernan CF, Frye CS, Demetris AJ, Feldman AM. Cardiac-specific overexpression of tumor necrosis factor-alpha causes lethal myocarditis in transgenic mice. J Card Fail. 1997; 3:117–124. [PubMed: 9220311]
6. Sun M, Chen M, Dawood F, Zurawska U, Li JY, Parker T, et al. Tumor necrosis factor-alpha mediates cardiac remodeling and ventricular dysfunction after pressure overload state. Circulation. 2007; 115:1398–1407. [PubMed: 17353445]
7. Popivanova BK, Kitamura K, Wu Y, Kondo T, Kagaya T, Kaneko S, et al. Blocking TNF-alpha in mice reduces colorectal carcinogenesis associated with chronic colitis. J Clin Invest. 2008; 118:560–570. [PubMed: 18219394]

8. Brzezinska-Blaszczyk E, Pietrzak A, Misiak-Tloczek AH. Tumor necrosis factor (TNF) is a potent rat mast cell chemoattractant. J Interferon Cytokine Res. 2007; 27:911–919. [PubMed: 18052723]
9. Murray DB, Gardner JD, Brower GL, Janicki JS. Effects of nonselective endothelin-1 receptor antagonism on cardiac mast cell-mediated ventricular remodeling in rats. Am J Physiol Heart Circ Physiol. 2008; 294:H1251–H1257. [PubMed: 18178727]
10. Dolgilevich SM, Siri FM, Atlas SA, Eng C. Changes in collagenase and collagen gene expression after induction of aortocaval fistula in rats. Am J Physiol Heart Circ Physiol. 2001; 281:H207–H214. [PubMed: 11406487]
11. Shijo H, Iwabuchi K, Hosoda S, Watanabe H, Nagaoka I, Sakakibara N. Evaluation of neutrophil functions after experimental abdominal surgical trauma. Inflamm Res. 1998; 47:67–74. [PubMed: 9535544]
12. Barbuio R, Milanski M, Bertolo MB, Saad MJ, Velloso LA. Infliximab reverses steatosis and improves insulin signal transduction in liver of rats fed a high-fat diet. J Endocrinol. 2007; 194:539–550. [PubMed: 17761893]
13. Li M, Naqvi N, Yahiro E, Liu K, Powell PC, Bradley WE, et al. c-kit is required for cardiomyocyte terminal differentiation. Circ Res. 2008; 102:677–685. [PubMed: 18258857]
14. Wagner RA, Tabibiazar R, Powers J, Bernstein D, Quertermous T. Genome-wide expression profiling of a cardiac pressure overload model identifies major metabolic and signaling pathway responses. J Mol Cell Cardiol. 2004; 37:1159–1170. [PubMed: 15572046]
15. Kolpakov MA, Seqqat R, Rafiq K, Xi H, Margulies KB, Libonati JR, et al. Pleiotropic effects of neutrophils on myocyte apoptosis and left ventricular remodeling during early volume overload. J Mol Cell Cardiol. 2009; 47:634–645. [PubMed: 19716828]
16. Rutschow S, Li J, Schultheiss HP, Pauschinger M. Myocardial proteases and matrix remodeling in inflammatory heart disease. Cardiovasc Res. 2006; 69:646–656. [PubMed: 16417902]
17. Sun M, Dawood F, Wen WH, Chen M, Dixon I, Kirshenbaum LA, et al. Excessive tumor necrosis factor activation after infarction contributes to susceptibility of myocardial rupture and left ventricular dysfunction. Circulation. 2004; 110:3221–3228. [PubMed: 15533863]
18. Roncon-Albuquerque R Jr, Vasconcelos M, Lourenco AP, Brandao-Nogueira A, Teles A, Henriques-Coelho T, et al. Acute changes of biventricular gene expression in volume and right ventricular pressure overload. Life Sci. 2006; 78:2633–2642. [PubMed: 16310223]
19. Bozkurt B, Kribbs SB, Clubb FJ Jr, Michael LH, Didenko VV, Hornsby PJ, et al. Pathophysiologically relevant concentrations of tumor necrosis factor-alpha promote progressive left ventricular dysfunction and remodeling in rats. Circulation. 1998; 97:1382–1391. [PubMed: 9577950]
20. Frangogiannis NG, Entman ML. Identification of mast cells in the cellular response to myocardial infarction. Methods Mol Biol. 2006; 315:91–101. [PubMed: 16110151]
21. Reil JC, Gilles S, Zahler S, Brandl A, Drexler H, Hultner L, et al. Insights from knock-out models concerning postischemic release of TNFalpha from isolated mouse hearts. J Mol Cell Cardiol. 2007; 42:133–141. [PubMed: 17101148]
22. Gordon JR, Galli SJ. Mast cells as a source of both preformed and immunologically inducible TNF-alpha/cachectin. Nature. 1990; 346:274–276. [PubMed: 2374592]
23. Wang BW, Hung HF, Chang H, Kuan P, Shyu KG. Mechanical stretch enhances the expression of resistin gene in cultured cardiomyocytes via tumor necrosis factor-alpha. Am J Physiol Heart Circ Physiol. 2007; 293:H2305–H2312. [PubMed: 17573461]
24. Dai RP, Dheen ST, He BP, Tay SS. Differential expression of cytokines in the rat heart in response to sustained volume overload. Eur J Heart Fail. 2004; 6:693–703. [PubMed: 15542404]
25. Yokoyama T, Sekiguchi K, Tanaka T, Tomaru K, Arai M, Suzuki T, et al. Angiotensin II and mechanical stretch induce production of tumor necrosis factor in cardiac fibroblasts. Am J Physiol. 1999; 276:H1968–H1976. [PubMed: 10362677]
26. Lantz CS, Boesiger J, Song CH, Mach N, Kobayashi T, Mulligan RC, et al. Role for interleukin-3 in mast-cell and basophil development and in immunity to parasites. Nature. 1998; 392:90–93. [PubMed: 9510253]
27. Kurrelmeyer KM, Michael LH, Baumgarten G, Taffet GE, Peschon JJ, Sivasubramanian N, et al. Endogenous tumor necrosis factor protects the adult cardiac myocyte against ischemic-induced

apoptosis in a murine model of acute myocardial infarction. Proc Natl Acad Sci U S A. 2000; 97:5456–5461. [PubMed: 10779546]

28. Hohensinner PJ, Kaun C, Rychli K, Niessner A, Pfaffenberger S, Rega G, et al. Macrophage colony stimulating factor expression in human cardiac cells is upregulated by tumor necrosis factor-alpha via an NF-kappaB dependent mechanism. J Thromb Haemost. 2007; 5:2520–2528. [PubMed: 17922812]
29. Tarzami ST, Calderon TM, Deguzman A, Lopez L, Kitsis RN, Berman JW. MCP-1/CCL2 protects cardiac myocytes from hypoxia-induced apoptosis by a G(alphai)-independent pathway. Biochem Biophys Res Commun. 2005; 335:1008–1016. [PubMed: 16102724]
30. Hamid T, Gu Y, Ortines RV, Bhattacharya C, Wang G, Xuan YT, et al. Divergent tumor necrosis factor receptor-related remodeling responses in heart failure: role of nuclear factor-kappaB and inflammatory activation. Circulation. 2009; 119:1386–1397. [PubMed: 19255345]
31. Jobe LJ, Melendez GC, Levick SP, Du Y, Brower GL, Janicki JS. TNF-alpha inhibition attenuates adverse myocardial remodeling in a rat model of volume overload. Am J Physiol Heart Circ Physiol. 2009; 297:H1462–H1468. [PubMed: 19666842]
32. Mann DL. Inflammatory mediators and the failing heart: past, present, and the foreseeable future. Circ Res. 2002; 91:988–998. [PubMed: 12456484]

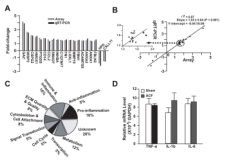

Figure 1. Microarray analysis and validation by qRT-PCR of 24 hour ACF

(A) Comparison of gene fold-change by microarray and qRT-PCR in 10% of the total altered genes identified by microarray. *Refers to supplemental Table 1 for gene annotation. **(B)** Correlation between expression changes by microarray vs. qRT-PCR with best-fit linear regression line. Inset - Genes with a 1.4-2-fold change plotted for better visibility. **(C)** Functional classification of genes (162) differentially expressed in ACF vs. Sham. **(D)** Relative expression of TNF-α, IL-1b (interleukin 1β) and IL-6 (interleukin 6) mRNA by qRT-PCR in ACF and sham.

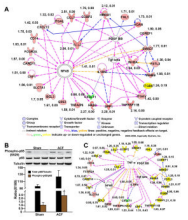

Figure 2. IPA analysis of differentially expressed genes in 24 hour ACF (see Table 2)

(A) IPA network of interactive genes involved in inflammation and immune response ($P < 10^{-56}$). Connecting line(s) represent known biological relation between genes. Fold-changes and P-value derived from qRT-PCR are listed beside each gene. **(B)** Western blot of phospho- and total NF-κB p65 in ACF vs. sham. Tubulin loading control. $^{*}P < 0.05$ vs. sham. **(C)** IPA analysis of the interaction between TNF-α and the identified gene network in **(A)**. Effect of TNF-α neutralization on each gene was determined by qRT-PCR (fold-change and P-value listed beside each gene).

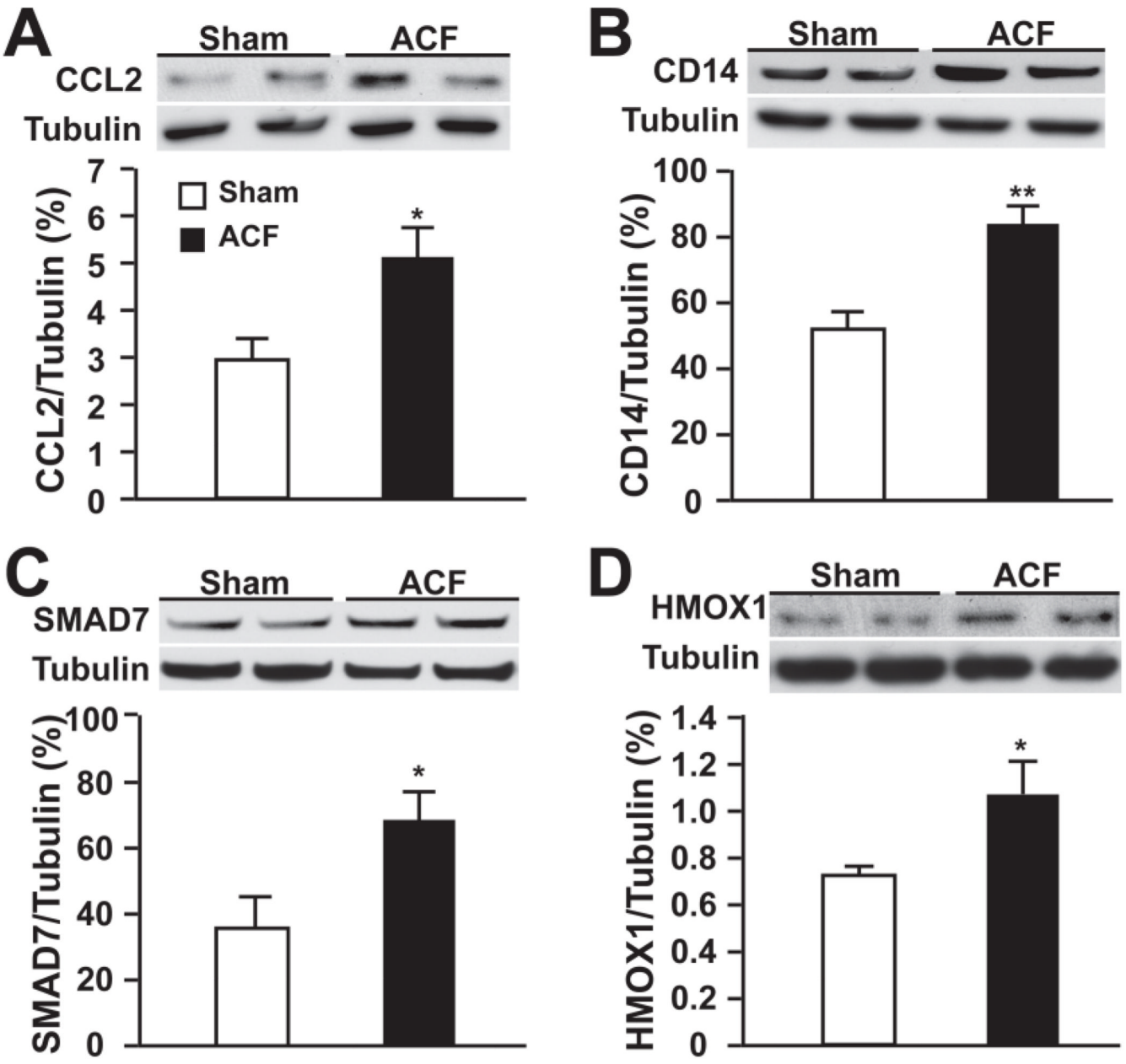

Figure 3. Representative western blot of TNF-α related inflammation proteins in IPA network

Expression of **(A)** CCL2 (chemokine (c-c) motif ligand 2), **(B)** CD14, **(C)** SMAD7 (SMAD family member 7) and **(D)** HMOX1 (heme oxygenase 1) in sham and ACF at 24 hours. Densitometric analysis after normalization to tubulin is presented below. **P* < 0.05, ***P* < 0.01 vs. sham.

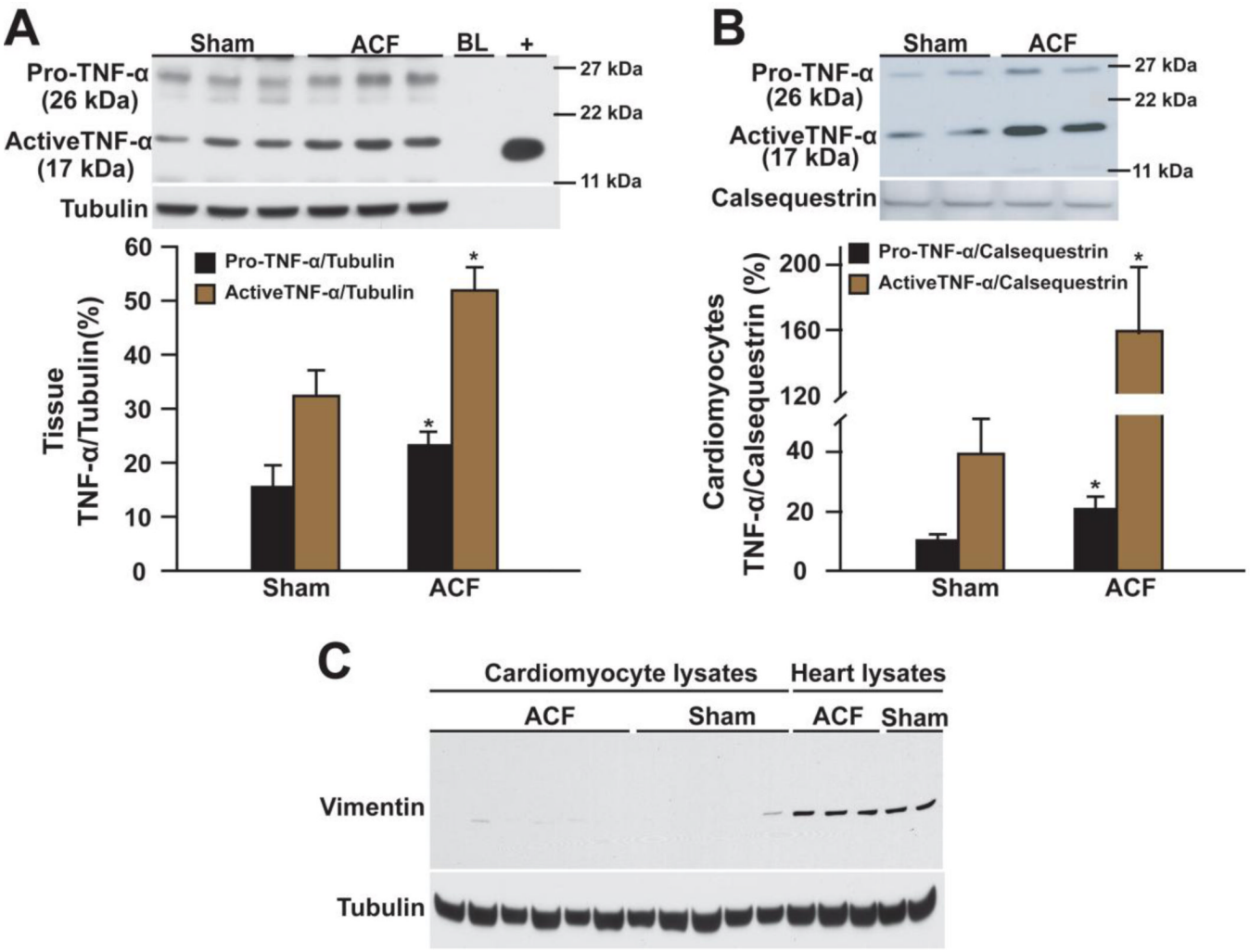

Figure 4. Western blot of TNF-α in LV tissue and isolated cardiomyocytes of 24 hour ACF

Pro- and active TNF-α in **(A)** heart lysates and **(B)** cardiomyocytes from ACF vs. shams. "**BL**" loading dye. "**+**" recombinant active rat TNF-α. Densitometric analysis is presented below. **P* < 0.05, ***P* < 0.01 vs. sham. **(C)** Western blot of vimentin in cardiomyocytes and heart lysates (positive for vimentin) to ensure the purity of cardiomyocytes. Tubulin or calsequestrin was used as loading control.

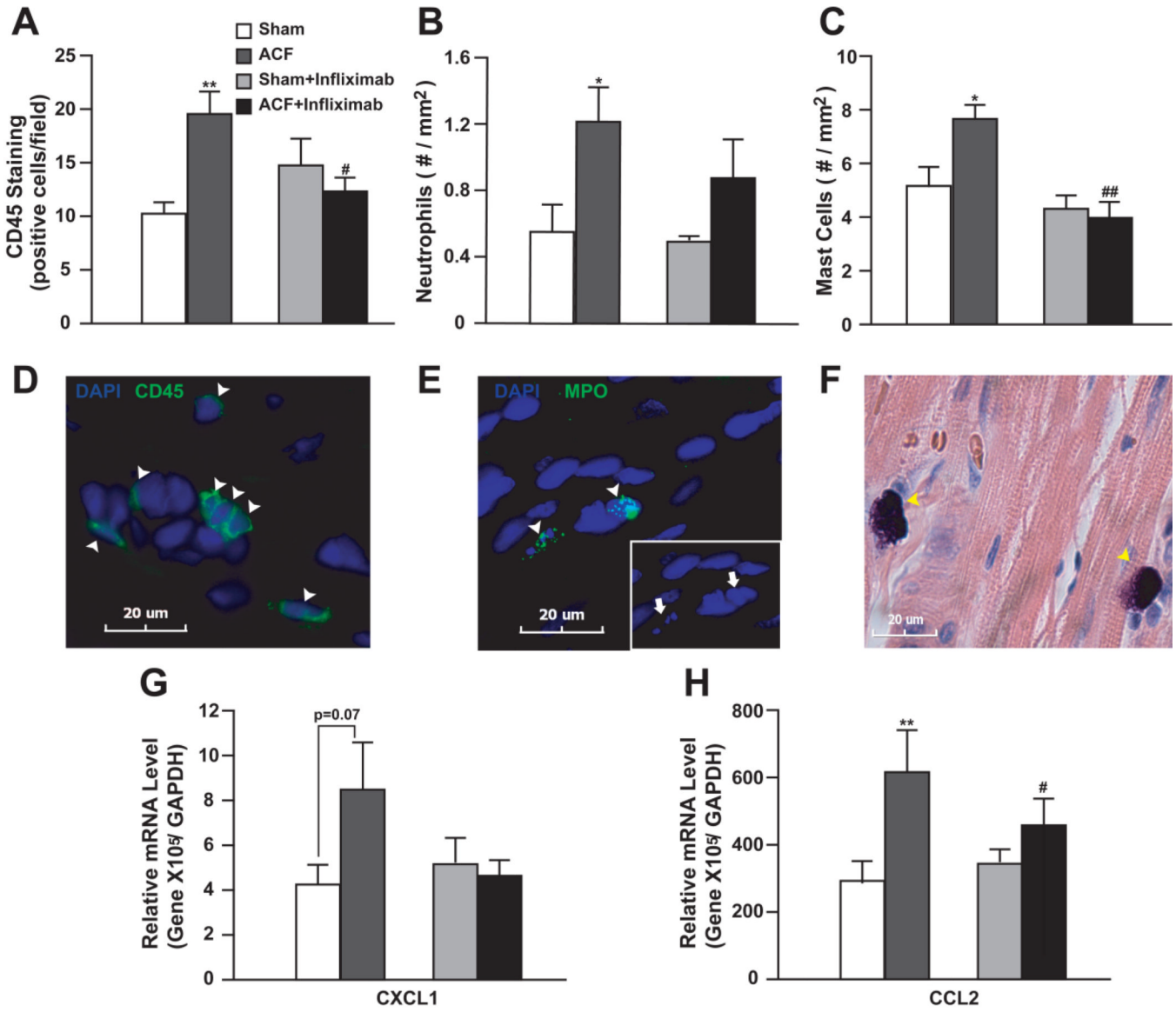

Figure 5. Effect of TNF-α neutralization (Infliximamb) on myocardial inflammatory response to 24 hour ACF

Number of **(A)** CD45+ cells, **(B)** neutrophils and **(C)** mast cells in ACF and shams with or without infliximab was quantified. Representative images of **(D)** CD45+ cells (green), **(E)** neutrophils with myeloperoxidase (MPO) staining (green), and **(F)** mast cells with Giemsa staining (purple) were shown below. Nuclei were stained blue with DAPI. Arrowheads indicate positively stained cells. Arrows in **(E)** demonstrate multilobular nuclei of neutrophils. **(G)** and **(H)** demonstrate relative CXCL1 and CCL2 mRNA levels quantified by qRT-PCR in ACF and shams with or without infliximab. Expression level was normalized to GAPDH. **P*<0.05, ***P*< 0.01 vs. sham; #*P*<0.05, ##*P*<0.01 vs. ACF.

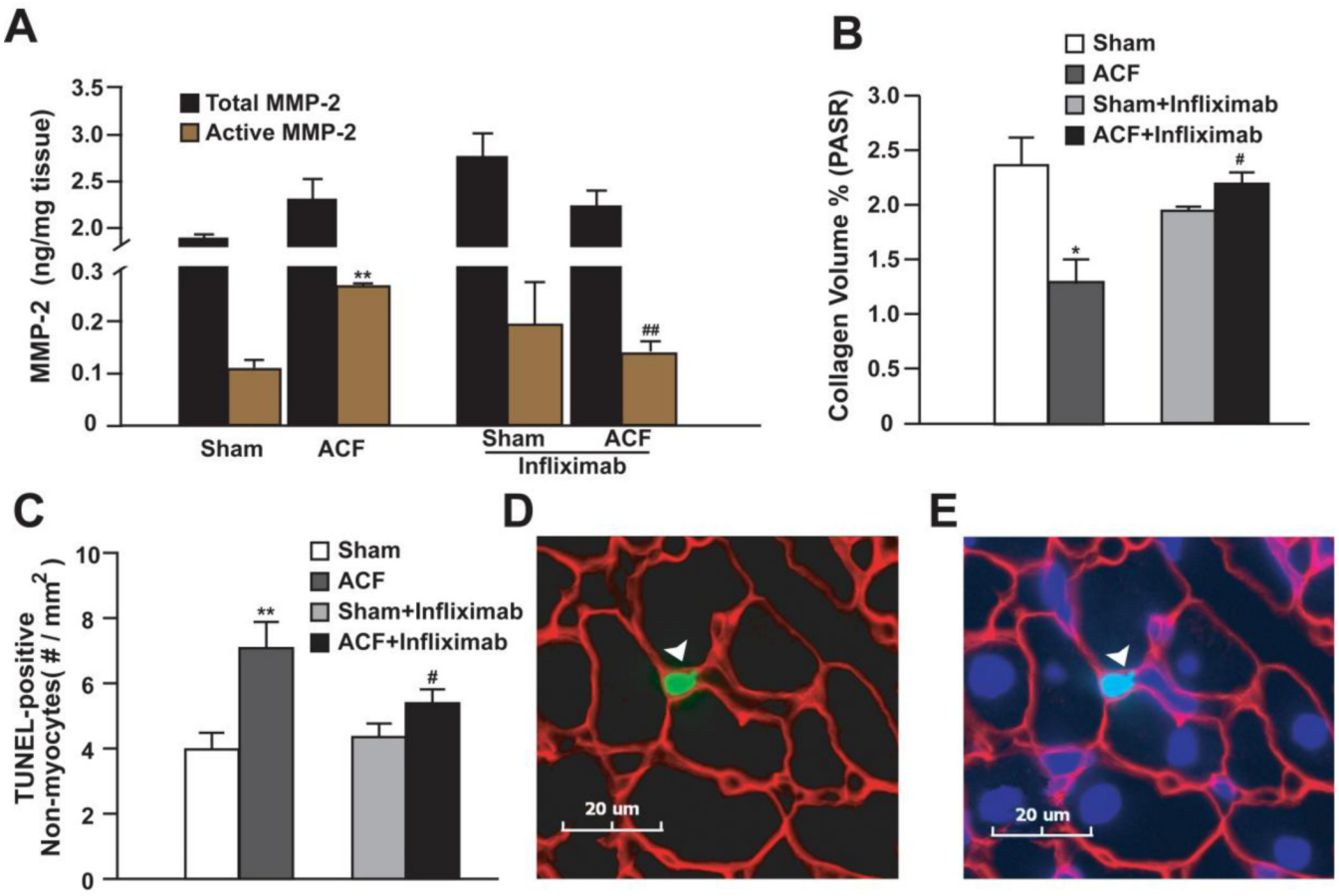

Figure 6. Effect of TNF-α neutralization on MMP-2, collagen and apoptosis in 24 hour ACF

(A) LV total and active MMP-2 and **(B)** interstitial collagen in ACF and sham rats with or without infliximab was quantified. **(C)** Quantification of TUNEL-positive non-myocyte nuclei in ACF and sham rats with or without infliximab. **(D)** Representative image of a TUNEL-positive non-cardiomyocyte nucleus (green - arrowhead) **(E)** also nuclear stained with DAPI (blue). Counter stain is laminin (red). **P*<0.05, ***P*< 0.01 vs. sham; #*P*<0.05, ##*P*<0.01 vs. ACF.

Table 1

LV hemodynamics and remodeling 24h after ACF or sham surgery with and without TNF-α blockade

	Vehicle		Infliximab	
	Sham	**ACF**	**Sham**	**ACF**
LV weight/BW, 10^{-3}	2.4±0.06	2.4±0.06	2.5±0.04	2.5±0.06
Lung weight, g	1.3±0.04	1.3±0.04	1.2±0.04	1.2±0.05
Heart rate, beats/min	383±10	379±17	391±15	374±9
LVEDP, mmHg	2.0±0.3	6.0±1.0*	1.3±0.3†	6.1±0.7*
LVESP, mmHg	57±2	49±2*	50±2†	39±2*#
LVEDD, mm	7.0±0.1	7.8±0.2*	7.3±0.2	7.9±0.3*
LVESD, mm	4.2±0.2	3.9±0.2	4.0±0.1	4.1±0.2
LV +dp/dt_{max}, mmHg/s	6890±281	6834±171	6076±268	5869±368
LV -dp/dt_{max}, mmHg/s	−6152±309	−5511±211	−5771±252	−4794±346*
LV FS, %	41±3	50±2*	45±2	48±4
LV VCFr	7.8±0.4	9.7±0.8*	7.9±0.6	8.6±0.7
n	5	5	6	5

Values are mean ± SEM.

*P <0.05 vs. corresponding sham,

†P <0.05 vs. untreated sham,

#P < 0.05 vs. ACF.

BW, body weight; LVEDP, Left ventricle end-diastolic pressure; LVESP, Left ventricle end-systolic pressure; LVEDD, LV end-diastolic dimension; LVESD, LV end-systolic dimension; FS, fractional shortening; VCFr, Velocity of circumferential wall shortening.

Table 2

Altered inflammation associated genes in the IPA network

Genes	Fold-Change*	P-value*	Description	Category	Access. #
CCL7	2.1	0.001	chemokine (c-c motif) ligand 7	chemokine	NM_001007612
CCL2	2.2	0.001	chemokine (c-c motif) ligand 2	chemokine	NM_031530
CXCL12	1.5	0.001	chemokine (c-x-c motif) ligand 12	chemokine	AF217564
CXCL11	−1.6	0.019	chemokine (c-x-c motif) ligand 11	chemokine	NM_182952
CSF1	1.6	0.002	colony stimulating factor 1	cytokine	NM_023981
IL1RN	1.7	0.009	interleukin 1 receptor antagonist	cytokine	NM_022194
SPP1	2.5	0.017	secreted phosphoprotein 1	cytokine	NM_012881
INHBA	1.5	0.050	inhibin, beta A	growth factor	NM_017128
INHBB	1.9	0.003	inhibin, beta B	growth factor	XM_344130
FSTL3	1.5	0.007	follistatin-like 3	activin inhibitor	NM_053629
SMAD7	1.5	0.003	SMAD family member 7	cell signaling	NM_030858
HAS2	2.7	0.001	hyaluronan synthase 2	enzyme	NM_013153
HMOX1	1.9	0.017	heme oxygenase 1	enzyme	NM_012580
CGREF1	1.9	0.048	cell growth regulatory gene 11	cell cycle	NM_139087
FHL1	1.8	0.013	four and a half LIM domains 1	cell cycle	BC061782
G0S2	1.5	0.015	G0/G1switch 2	cell cycle	NM_001009632
CARD11	1.5	0.018	caspase recruitment domain 11	kinase	XM_001073551
VCAN	2.3	0.010	Versican	ECM#	XM_001058160
TNFAIP6	1.8	0.010	TNF-alpha induced protein 6	ECM binding	XM_001065494
ITGAV	1.5	0.005	integrin, alpha V	ECM receptor	XM_230950
ITGB6	1.9	0.004	integrin, beta 6	ECM receptor	NM_001004263
ITGAL	1.6	0.016	integrin alpha L	ECM receptor	XM_219349
CCBP2	1.8	0.021	chemokine binding protein 2	receptor	NM_078621
CD14	1.8	0.001	CD14 molecule	receptor	NM_021744
FCGR2A	2.0	0.037	CD32	receptor	XM_001077008
TNFRSF11B	2.2	0.012	osteoprotegerin	receptor	NM_012870
BCL3	1.5	0.007	B-cell CLL/lymphoma 3	transcription	XM_001057993
SLC7A1	1.6	0.019	solute carrier family 7 member 1	transporter	NM_013111

* fold changes and P-values from microarray analysis.

ECM: extracellular matrix protein